Carbohydrate Polymers 84 (2011) 186–194

Contents lists available at ScienceDirect

Carbohydrate Polymers

journal homepage: www.elsevier.com/locate/carbpol

Effect of citrate spacer on mucoadhesive properties of a novel water-soluble cationic β-cyclodextrin-conjugated chitosan

Saowaluk Chaleawlert-umpon, Onanong Nuchuchua, Somsak Saesoo, Pattarapond Gonil, Uracha Rungsardthong Ruktanonchai, Warayuth Sajomsang, Nuttaporn Pimpha*

National Nanotechnology Center, National Science and Technology Development Agency, Pathumthani 12120, Thailand

ARTICLE INFO

Article history:
Received 30 June 2010
Received in revised form 7 November 2010
Accepted 10 November 2010
Available online 21 November 2010

Keywords:
β-Cyclodextrin-conjugated chitosan
Citrate spacer
Mucoadhesivity
Surface plasmon resonance
Mucoadhesive drug delivery system

ABSTRACT

β-Cyclodextrin (CD) was designed to conjugate with chitosan (CS) through citrate spacer in order to facilitate mucoadhesive properties and CD mobility. To improve their water solubility, the CS backbones were further quaternized with glycidyl trimethylammonium chloride. The mucoadhesive properties of CD-conjugated CS derivatives evaluated by mucin-particle method and surface plasmon resonance sensor were found to be depend on degree of quaternization and citrate amount. The electrostatic attraction between positively charged amino groups of the cationic CS and the negatively charged of the mucin as well as hydrogen bonding between carboxyl and hydroxyl groups of citrate spacers and mucus glycoprotein presumably mediated the mucoadhesion. Moreover, the cytotoxicity test indicated that the CD-conjugated CS derivatives resulted in less toxicity against buccal mucosal cells than the original quaternized CS. Therefore, the CD-conjugated CS derivatives could be useful for mucoadhesive drug delivery systems.

1. Introduction

Nowadays, mucoadhesive polymers, which are capable of attaching to mucosal surfaces, have received much attention as promising drug carriers. Since they can prolong the residence time at the site of drug absorption, the improved specific localization of drug delivery on mucus membrane could be possibly attained (Ludwig, 2005; Salamat-Miller, Chittchang, & Johnston, 2005; Ugwoke, Agu, Verbeke, & Kinget, 2005). The attachment of mucoadhesive polymers to the membrane occurs through interpenetration/interdiffusion of polymers and substrates, and is followed by non-covalent bonding i.e., electrostatic interaction and hydrogen bonding (Andrews, Laverty, & Jones, 2009; Huang, Leobandung, Foss, & Peppas, 2000; Serra, Doménech, & Peppas, 2009). Therefore, polymeric components play an important role in diffusion, entanglement, and mucoadhesion. Modification and control of polymer properties are beneficial for specific tailoring of polymer–mucus interactions.

Among the mucoadhesive polymers, chitosan (CS), a β-(1,4)-linked polysaccharide of D-glucosamine, has attracted great attention, since it possesses interesting properties such as biocompatibility, biodegradability, and a cationic charge in acidic condition (Cardile et al., 2008; Lehr, Bouwstra, Schacht, & Junginger, 1992). Moreover, CS provides primary amine groups at C-2 position and hydroxyl groups at C-6 position, which are capable of attaching to the mucosal surface through chemical bonding. Despite the effective properties of CS in mucosal interaction and targeting, there are still some drawbacks with respect to its insolubility in water under neutral or alkaline condition and poor hydrophobic drugs loading. To overcome these problems, many approaches have emerged to suggest the modification (Gomes, Gomes, Batista, Pinto, & Silva, 2008; Snyman, Hamman, Kotze, Rollings, & Kotzé, 2002; Thanou et al., 2000; Trapani, Sitterberg, Bakowsky, & Kissel, 2009), and incorporatation of the cyclodextrin moieties into CS backbones (Prabaharan & Jayakumar, 2009; Teijeiro-Osorio, Remuñán-López, & Alonso, 2009; Zhang et al., 2009). Cyclodextrins, a class of cyclic oligosaccharides with six to eight D-glucose units linked by 1,4-glucosidic bonds, have been investigated as a good candidate, as they are able to complex a variety of hydrophobic compounds via a host–guest inclusion complexation (Liu & Zhu, 2007; Marques, Hadgraft, & Kellaway, 1990). Grafting cyclodextrin molecules into CS backbone therefore results in a mucoadhesive delivery systems, having cumulative effects of inclusion, bioavailability improvement, and specific mucosal targeting (Prabaharan & Mano, 2006).

A covalent attachment of cyclodextrin into CS backbones is mostly based on an amidation of cyclodextrin bearing carboxylic acid and CS (El-Tahlawy, Gaffar, & El-Rafie, 2006) with the aid of 1-ethyl-3-(3-dimethylaminopropyl) carbodiimide (Furusaki,

* Corresponding author at: National Nanotechnology Center, 113 Thailand Science Park, Pahonyothin Rd., Klong 1, Klong Luang, Phathumthani 12120, Thailand. Tel.: +66 2564 7100x6551; fax: +66 2564 6981.
E-mail address: nuttaporn@nanotec.or.th (N. Pimpha).

0144-8617/$ – see front matter © 2010 Elsevier Ltd. All rights reserved.
doi:10.1016/j.carbpol.2010.11.017

Ueno, Sakairi, Nishi, & Tokura, 1996; Krauland & Alonso, 2007). Cyclodextrin-grafted CS was also prepared by a nucleophilic substitution of cyclodextrin, containing reactive groups such as chloro and tosyl groups, with primary amine groups of CS (Chen & Wang, 2001; Martel et al., 2001). Aldehyde-containing cyclodextrin was useful to graft into CS via Schiff's base formation, which is subsequently reduced to amine (Tojima et al., 1998; Venter, Kotzé, Auzély-Velty, & Rinaudo, 2006). Crosslinkers, e.g., 1,6-hexamethylene diisocyanate, were utilized to link hydroxyl groups of both cyclodextrin and CS together under low pH value (Chiu, Chung, Giridhar, & Wu, 2004; Zha, Li, & Chang, 2008). Grafting copolymerization of cyclodextrin bearing vinyl groups and CS was conducted with redox initiators, such as ceric ammonium nitrate and potassium persulfate (Gaffar, El-Rafie, & El-Tahlawy, 2004). Besides cyclodextrin modification, CS was activated with epoxy to prepare a reactive CS, which underwent ring opening with sulfonated cyclodextrin (Zhang, Wang, & Yi, 2004). Despite the success of preparation, its poor solubility in water under neutral or alkaline condition has prevented its utilization, particularly in pharmaceutical applications.

To address this problem, we designed a novel water-soluble cationic β-cyclodextrin-grafted chitosan for mucoadhesive drug delivery systems. CS was conjugated with β-cyclodextrin (CD) and subsequently quaternized with glycidyl trimethylammonium groups. Citric acid was utilized as a spacer in order to facilitate CD mobility. Since the structure of citrate spacer has many hydrogen bond forming groups such as hydroxyl and carboxyl groups, which may promote the mucoadhesive interaction, the effect of citrate spacer on mucoadhesive properties was therefore verified by mucin-particle and surface plasmon resonance (SPR) methods. The in vitro cytotoxicity of CS bearing CD derivatives against buccal mucosal cells was also investigated.

2. Materials and methods

2.1. Materials

The following materials were of analytical grade and used without further purification. Chitosan (CS) was purchased from Seafresh (Thailand). The weight-average molecular weight of CS was approximately 22 kDa, determined by a solution viscosity method. The degree of deacetylation was ca. 94%, as estimated by ^{1}H NMR spectroscopy (Hirai, Odani, & Nakajima, 1991). β-Cyclodextrin (CD) was obtained from Wacker (USA). Citric acid (CA), glycidyl trimethylammonium chloride (GTMAC), *N*-hydroxysuccinimide (NHS), and 1-ethyl-3-(3-dimethylaminopropyl) carbodiimide hydrochloride (EDC) were obtained from Fluka (Switzerland). Mucin (type III) from porcine and poly(acrylic acid) (PAA, Mw ~140 kDa) were purchased from Sigma–Aldrich (USA). Water used for all experiments was deionized from MilliQ Plus (Millipore, Schwalbach, Germany). Dulbecco's modified Eagle's medium (DMEM) and F12 were purchased from GIBCO (Invitrogen, USA). Fetal bovine serum (FBS) was received from Biochrom AG (Germany). Amphotericin B, L-glutamine, penicillin G sodium, streptomycin sulfate, and 3-(4,5-dimethylthiazol-2-yl)-2,5-diphenyl-tetrazolium bromide were purchased from Sigma–Aldrich (USA).

2.2. Synthesis of CD citrate (CDCA)

The CDCA was synthesized based on a reported method with minor modification (El-Tahlawy et al., 2006). CA (3.5 mmol, 0.68 g) was dissolved in water (1.2 mL), and followed by the addition of CD (1.76 mmol, 2 g). The molar ratio of carboxylic acid groups from CA to hydroxyl groups from CD was calculated to be 1:1. The reaction mixture was refluxed at 100 °C for 3 h, and isopropanol (*i*PrOH) was added to precipitate the product. The resulting precipitant was purified by soxhlet extraction with *i*PrOH to remove CA residues.

FTIR (KBr): 3349 (br, OH), 2919 (s, CH), 1718 (s, C=O), 1024 cm^{-1} (s, C–O). ^{1}H NMR (D_2O): δ = 2.74 (dd, C$\underline{H}_2$ of citrate moiety, J_{HH} = 15.6 Hz), 3.92–3.48 (m, H^2–H^6), 5.01 (s, H^1).

2.3. Synthesis of CDCA-grafted CS (CDCA-g-CS)

The CDCA-*g*-CS was prepared by amide formation between amine groups of CS and free carboxyl groups of CDCA. CS (24 mmol, 4 g) was added in 50 mL of 1% acetic acid solution overnight to allow the CS to completely dissolve. After that, 140 mL of CDCA (30 mmol, 40 g) solution was introduced to CS solution and refluxed at 130 °C for various time intervals to manipulate the grafting percentages. Then, the reaction mixture was cooled down to room temperature, followed by the addition of 200 mL of NaOH solution (0.2 M) to precipitate the grafted product. The obtained precipitant was subsequently purified by placing into a dialysis bag with a 12 kDa molecular weight cutoff (Cellu Sep T4) and dialyzed against distilled water. The water medium was changed daily for 3 days at room temperature until the conductivity of water was comparable to that of the purified H_2O used.

FTIR (KBr): 3374 (br, OH), 2883 (s, CH), 1753 (s, C=O), 1636 (s, NH), 1373 (s, CN), 1067 cm^{-1} (s, C–O). ^{1}H NMR (D_2O with acetic acid-d_4): δ = 1.92 (s, C$\underline{H}_3$ of *N*-acetylated glucosamine units), 2.67 (dd, C$\underline{H}_2$ of citrate moiety, J_{HH} = 15.6 Hz), 3.03–2.99 (m, H$^{2\prime}$), 3.82–3.30 (m, H^2–H^6 and H$^{3\prime}$–H$^{6\prime}$), 5.01–5.00 (m, H^1 and H$^{1\prime}$).

The grafting percentage and grafting efficiency (GE) were calculated by ^{1}H NMR spectroscopy and gravimetric analysis according to the following equations:

$$\text{Grafting}(\%) = \left[\frac{(I_a/4)}{I_{H^{2\prime}}}\right] \times 100 \quad (1)$$

$$\text{GE}(\%) = \left[\frac{W_g}{W_{CD} + W_{CS}}\right] \times 100 \quad (2)$$

where I_a is the integral peak area of methylene protons from citrate moiety (represented as 'a'), $I_{H^{2\prime}}$ is the integral peak area of H$^{2\prime}$ from glucosamine units, and W_g, W_{CD} and W_{CS} are the weights of CDCA-*g*-CS, CDCA and CS, respectively.

2.4. Synthesis of cationic CDCA-g-CS (QCDCA-g-CS)

The CDCA-*g*-CS (9.4 mmol) was dissolved in 50 mL of 1% acetic acid solution overnight to yield a homogeneous solution. GTMAC, calculated to be three times more than the residue glucosamine units of CDCA-*g*-CS, was subsequently added into the solution. Thereafter, the mixture was heated at 50–60 °C for 20–22 h. The obtained product was purified by dialysis using a bag with a 12 kDa molecular weight cutoff against distilled water for 3 days at room temperature until the conductivity of water was close to that of purified H_2O used. For comparison, the cationic CS (QCS) without CD was also prepared under the same conditions.

FTIR (KBr): 3342 (br, OH), 2883 (s, CH), 1753 (s, C=O), 1636 (s, NH), 1404 (s, NH_3^+), 1067 cm^{-1} (s, C–O). ^{1}H NMR (D_2O): δ = 1.98 (s, C$\underline{H}_3$ of *N*-acetylated glucosamine units), 2.79–2.40 (m, H$^{2\prime}$, C$\underline{H}_2$CHOHCH$_2$, and C$\underline{H}_2$ of CDCA moiety), 3.07 (s, N(C$\underline{H}_3$)$_3$Cl), 4.16–3.21 (m, H^2–H^6, H$^{3\prime}$–H$^{6\prime}$, and C$\underline{H}_2$N(CH$_3$)$_3$Cl), 4.40 (s, CH$_2$C$\underline{H}$OHCH$_2$), 4.93–4.92 (m, H^1 and H$^{1\prime}$).

2.5. Characterization

FTIR spectra were recorded on Perkin Elmer System 2000R FTIR spectrophotometer in the range of 4000 and 400 cm^{-1} using KBr disk. ^{1}H NMR spectroscopic determinations were performed

on NMR spectroscopy (Advance AV 500 MHz, Bruker, USA), using D_2O or a mixture of D_2O/acetic acid-d_4 as the solvents. The crystallographic structures were analyzed by X-ray diffractometer (JDX-3530, JEOL, USA) using a $Cu_{K\alpha 1}$ lamp at $\lambda = 1.5405$ Å. The 2θ range used in the measurement was 4–40° in step of 0.02°. Differential scanning calorimeter (DSC) was conducted to study the thermal properties of the obtained products. DSC thermograms were recorded with differential scanning calorimeter (DSC823e/700, Mettler Toledo, Switzerland). The instrument was calibrated with an Indium standard under nitrogen atmosphere. Heating rate was carried out at 10 °C/min in the temperature range of 0 °C to 300 °C. Hydrodynamic diameter and polydispersity index (PDI) of mucin particles were measured using a dynamic light scattering (DLS) method with a zetasizer (NanoZS 4700, Malvern Instruments, UK) at 25 °C. The surface charge of mucin particles was measured by electrophoretic light scattering (ELS), using zetasizer (NanoZS 4700, Malvern Instruments, UK) at room temperature. The measurements were done at a wavelength of 633 nm at 25 °C with a scattering angle of 90°. The results reported were the mean of three determinations. To evaluate the water solubility of QCDCA-*g*-CSs, the transmittance of the polymer solutions was acquired by UV–visible spectroscopy as a function of the polymer concentration. The dried polymer was accurately weighed and dissolved in 5 mL of distilled water in range of 0.01–1.0 mg/mL. The polymer solution was then stirred with magnetic stirrer at room temperature for 30 min. The transmittance of the solution was measured at 600 nm by UV–visible spectroscopy (Lambda 650, Perkin Elmer, USA), using a quartz cell with an optical path length of 1 cm. The solution is assigned as insoluble when the transmittance of the solution is less than 50% of the deionized water's transmittance (Cho, Grant, Piquette-Miller, & Allen, 2006).

2.6. Evaluation of mucoadhesive interaction of polymers on mucin

2.6.1. Mucin-particle method

Mucoadhesive properties of QCS and QCDCA-*g*-CS derivatives were determined using the mucin-particle method (Takeuchi et al., 2005; Thongborisute & Takeuchi, 2008). Prior to the experiment, submicron-sized mucin suspension (1%, w/v) was prepared by suspending and continuously stirring mucin type III powder in 0.38 mM Tris base pH 6.8 for 10 h. Mucin suspension was then incubated at 37 °C overnight. The mucin particle size was reduced by ultrasonication (VCX750, Sonics & Materials, Inc., USA), until the size of the particle was in a range of 200–300 nm. It was then centrifuged at 4000 rpm for 20 min to extract submicron-sized mucin particles in the supernatant portion. The average particle size was 250 ± 28 nm with narrow size distribution. The zeta-potential value of the obtained mucin was -12.5 ± 1.6 mV.

One milliliter of 1 (%w/v) mucin suspension was mixed with different concentrations of 0.05–0.35 (%w/v) polymer solutions under a mild magnetic stirring at room temperature. Then, the changes in mucin particle size and surface charge were monitored using DLS, and ELS methods. The QCS, and PAA were assigned as positive and negative controls, respectively.

2.6.2. Surface plasmon resonance (SPR) method

The mucoadhesive properties were further determined by SPR method, which was modified from the BIACORE method (Takeuchi et al., 2005; Thongborisute & Takeuchi, 2008). CMD500 (carboxymethyldextran hydrogel, XanTec bioanalytics GmbH, Germany) sensor chip surface was pre-activated with a mixture of 100 mM NHS and 400 mM EDC. Mucin particles at a concentration of 0.1% (w/v) were prepared in 10 mM acetate buffer (pH 4.5). All immobilizations were carried out at a flow rate of 50 μL/min. Firstly, CS was injected at a concentration of 0.1% (w/v) across the activated surface for 10 min. The remaining reactive esters were transformed into inactive amides by injection of 1 M ethanolamine hydrochloride, pH 8.5. Thereafter, the mucin particle suspension was injected and the baseline was recorded until equilibrium. Afterwards, the polymer solutions were injected for 10 min, ensuring a complete equilibrium. The refractive index unit (RIU) for each polymer was then recorded on the home-built SPR imaging system equipped with a 7-channel flow-cell. Details of the SPR imaging apparatus, similar to the system previously reported (Shumaker-Parry, Ruedi, & Campbell, 2004), were briefly discussed here. The collimated light beam from an 880-nm light emitting diode (LED) was passed through a linear polarizer and an iris aperture and then illuminated the functionalized SPR sensor chip through a BK7 prism in a Kretschmann configuration. The reflected images from the SPR chip were collected by a near-infrared CCD camera at the imaging angle which was adjusted in a linear region of the SPR curve to get the highest image contrast.

2.7. In vitro cytotoxicity study

Cell cytotoxicity of QCS and QCDCA-*g*-CS derivatives was attained on buccal mucosa cells (JCRB0831), obtained from Japanese Collection of Research Bioresources. The cells were grown in DMEM supplemented with 50% F12 medium, 10% FBS, 2 mM L-glutamine, penicillin G sodium, streptomycin sulfate and amphotericin B at 37 °C in a fully humidified, 5% CO_2. The cells were seeded in a 96-well plate at a density of 8000 cells/well and incubated for 24 h. The serial dilutions of sample (in a range of 0.05–20 mg/mL) were added to the cells and incubated for another 24 h. The cells were then tested with 3-(4,5-dimethylthiazol-2-yl)-2,5-diphenyltetrazolium bromide (MTT) assay. The MTT in PBS (0.5 mg/mL) was added to each well and the cells were incubated for 4 h. Medium and MTT were then aspirated from the wells, and formazan crystal was solubilized with 100 μL of DMSO. The absorbance was read with a microplate reader (SpectroMAX, USA) at a wavelength of 540 nm. The data were analyzed to determine the number of cell in each sample. The average of 8 wells was used to determine the mean of each point. Results were recorded as percentage absorbance relative to untreated control cells. The cytotoxicity results were used to calculate % relative cell viability after incubation with the samples as follows:

$$\%\text{Relative cell viability} = \frac{abs_{\text{sample}} - abs_{\text{DMSO}}}{abs_{\text{control}} - abs_{\text{DMSO}}} \times 100 \quad (3)$$

where abs_{sample} is the absorbance in a well containing sample, abs_{control} is the absorbance for untreated control cells, and abs_{DMSO} is the absorbance of DMSO.

IC_{50} values were extrapolated to 50% relative cell viability using linear regression analysis where the value can be obtained as the concentration of the polymers that is required to reduce the absorbance of cell viability to 50%.

3. Results and discussion

3.1. Synthesis of CDCA

The QCDCA-*g*-CS derivatives were synthesized through three steps: esterification of CD with citric acid, grafting onto CS, and quaternization with GTMAC as shown in Fig. 1. Considering the CD inclusion complexes, many findings reported that the steric hindrance effect due to substitution of CD plays a key role on the association constant of complexes (Prabaharan & Mano, 2006; Venter et al., 2006). In general, the incorporation of a guest molecule involves the wider secondary hydroxyl groups side of CD. Therefore, the primary hydroxyl group side was then suitable for conjugating with citric acid in the present study. Upon heating of citric acid, the

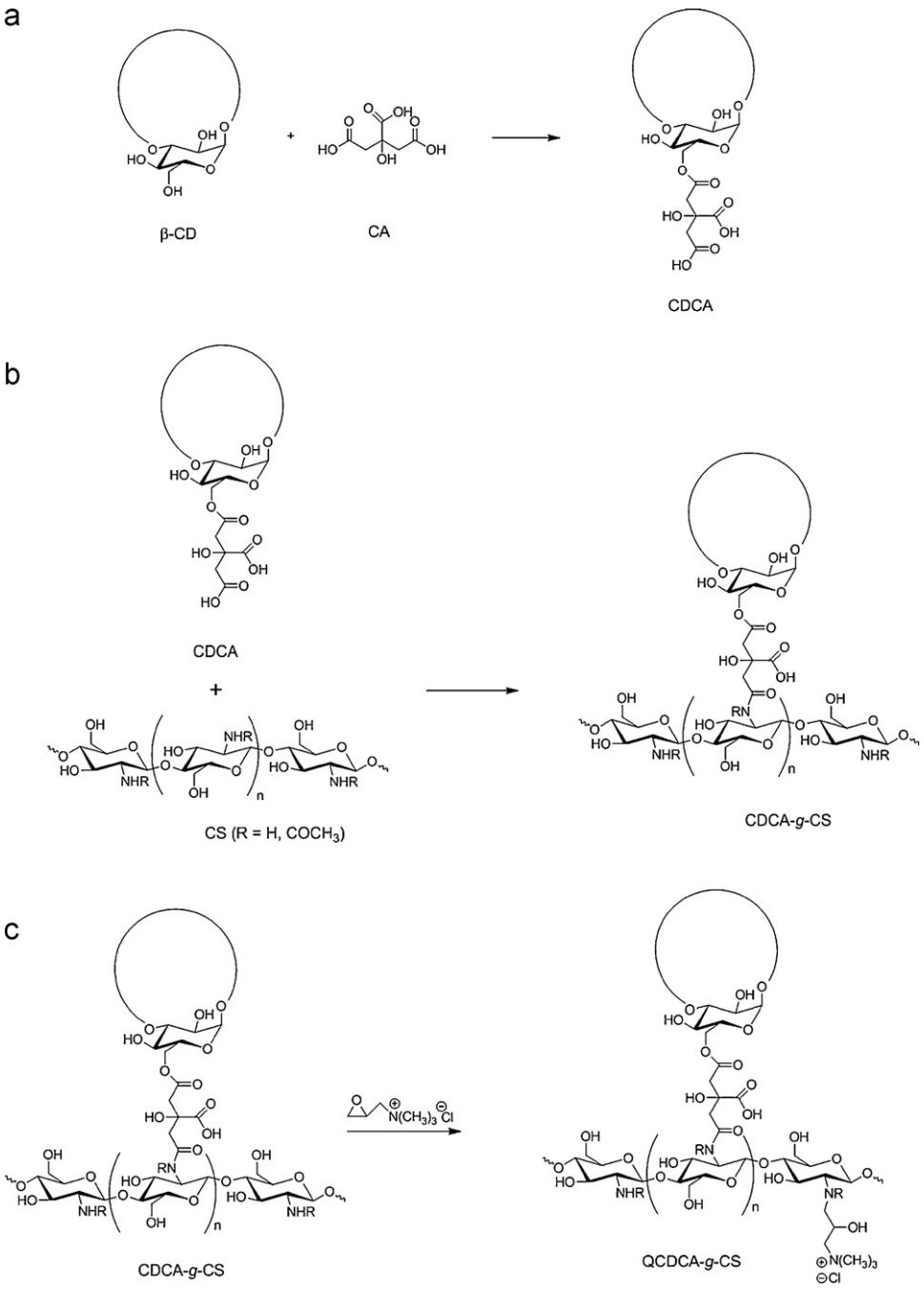

Fig. 1. Synthetic partway of cationic β-cyclodextrin-*g*-chitosan.

reactive cyclic anhydride intermediate was generated via a dehydration of the adjacent carboxyl groups. Once CD was introduced into the system, the reactive intermediate was reacted immediately with basic hydroxyl groups of CD. The most basic was the primary hydroxyl groups located on the C-6 of the glucopyranose units. The substitution therefore predominantly took place at the primary hydroxyl side of CD. The CDCA product was purified by precipitation and soxhlet extraction with *i*PrOH, resulting in a white solid product.

FTIR and ^{1}H NMR spectroscopy were used to confirm the presence of the product's functional groups. Fig. 2 shows the FTIR spectra of CD, CS, and their derivatives. The spectrum of original CD presented the strong absorption band at 3368 cm^{-1} assigned to O–H stretching. The characteristic peaks of CD at 1017 and 2903 cm^{-1} related to the C–O, and C–H stretching were also detected. By comparing the transmittance spectra of CD and CDCA, an additional absorption peak at 1718 cm^{-1} attributed to C=O stretching of citrate moieties was clearly observed. This additional peak was in good agreement with the ^{1}H NMR analysis in Fig. 3a, showing the ^{1}H NMR spectrum of CDCA. The multiplet peak at 3.48–3.92 ppm (H^2–H^6) and a singlet proton at 5.01 ppm (H^1) of CD were observed. In comparison with CD, CDCA exhibited an additional peak of a doublet of doublet at 2.74 ppm, which was associated with methylene protons of citrate moieties (represented as 'a'). It should be noted that these methylene protons of CDCA provided the doublet of doublet pattern, while the citric acid one exhibited a singlet peak, corresponding to the symmetric methylene protons.

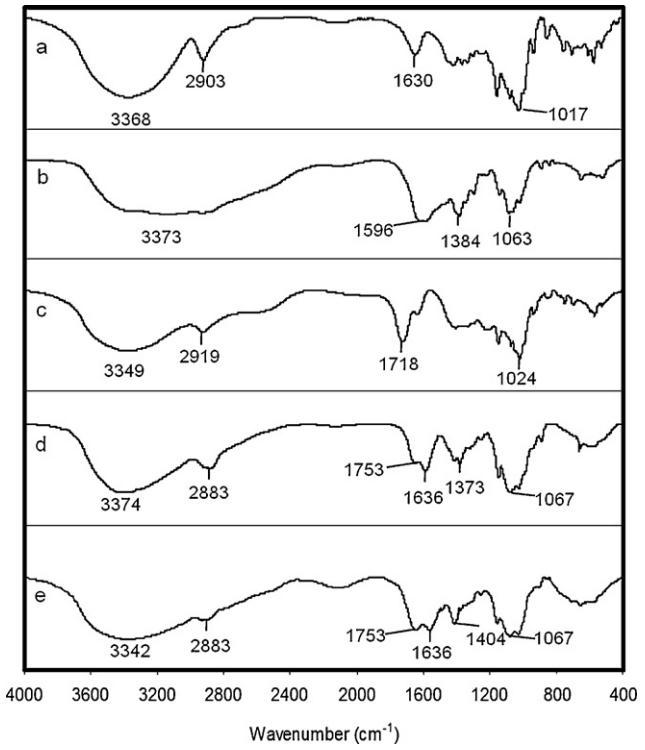

Fig. 2. FTIR spectra of (a) β-cyclodextrin, (b) chitosan, (c) β-cyclodextrin citrate, (d) β-cyclodextrin-*g*-chitosan at 22% grafting, and (e) cationic β-cyclodextrin-*g*-chitosan at 22% grafting.

3.2. Synthesis of CDCA-*g*-CS

CDCA was subsequently grafted onto CS through the amide formation between the amino groups of CS and the free carboxyl groups of CDCA. The influence of reaction time on grafting percentage was investigated. Increasing reaction time resulted in enhancing of grafting percentage. In this study, CDCA-*g*-CS at grafting percentage of 22, and 36, denoted as CDCA22-*g*-CS and CDCA36-*g*-CS, were selected for further investigation.

The constituent functional groups and grafting percentage were determined by FTIR and ^{1}H NMR spectroscopy. The FTIR spectrum of 94% deacetylated CS (Fig. 2b) showed the broad peak at 3600–3000 cm^{-1}, attributed to O–H stretching and N–H stretching. The absorption bands at 1063–1020 cm^{-1} (C–O stretching) and at 1596 and 1384 cm^{-1} (C=O of amide I and II) were the characteristic peaks of CS. CDCA-*g*-CS demonstrated the carbonyl absorption peak at 1753 cm^{-1} in addition to the original CS, which was associated to the citrate moieties at the spacer.

Fig. 3 shows ^{1}H NMR data of CDCA-*g*-CS compared to those of CDCA. The multiplet peak at 3.30–3.82 ppm was attributed to $H^{3'}$–$H^{6'}$ of glucosamine moieties and H^2–H^6 of glucopyranose moieties. The multiplet peak at 5.00–5.01 ppm was corresponded to H^1 of glucopyranose and $H^{1'}$ of glucosamine moieties, the multiplet peak at 2.99–3.03 ppm assigned to $H^{2'}$ of glucosamine units. It should be noted that the doublet of doublet peak of methylene protons from citrate moieties was shifted from 2.74 to 2.67 ppm after grafting. Based on FTIR and ^{1}H NMR analysis, we can draw a conclusion that CDCA was successfully grafted onto CS backbone via an amide formation.

The grafting percentage was calculated by ^{1}H NMR spectroscopic results, based on the additional citrate moieties per glucosamine units. Increasing reaction time from 4 to 8 h enhanced the grafting percentage from 22 to 36%.

Based on gravimetric analysis, grafting efficiency of CDCA22-*g*-CS and CDCA36-*g*-CS was 18 and 12%, respectively. The low efficiency was probably due to the competing interaction of acetic acid (solvent) rather than CDCA for amide formation. This behavior was also reported by El-Tahlawy et al. (2006).

3.3. Synthesis of QCDCA-*g*-CS

Although CD was successfully grafted onto CS backbone using citrate as the spacer, the application was still limited due to its insolubility at neutral or basic condition. The quaternization of CDCA-*g*-CS was, therefore, carried out to improve the CDCA-*g*-CS solubility using GTMAC as quaternary ammonium salt. The GTMAC was protonated in an acidic condition and its ring opening with amine groups on glucosamine moiety was then taken place. The quaternization of CDCA22-*g*-CS and CDCA36-*g*-CS were represented as QCDCA22-*g*-CS and QCDCA36-*g*-CS, respectively. The parent CS was also conjugated with GTMAC, denoted as QCS, which was also assigned as the control in the mucoadhesive test. Theoretically, degree of quaternization (DQ) should be equivalent to the residue reactive primary amine groups of glucosamine unit after CD grafting (i.e., primary amine groups = 72% for CDCA22-*g*-CS, and 58% for CDCA36-*g*-CS). Therefore, DQ values of QCS, QCDCA22-*g*-CS, and QCDCA36-*g*-CS were 94, 72, and 58%, respectively.

Fig. 2d shows the FTIR spectrum of QCDCA-*g*-CS. The presence of characteristic absorption peak at 1404 cm^{-1} and the broad band around 3342 cm^{-1} can be assigned to the additional quaternary ammonium and hydroxyl groups of the quaternary ammonium substitutent (Zhang et al., 2009). The ^{1}H NMR spectrum of QCDCA-*g*-CS was presented in Fig. 3c. The signals at 3.07, 3.63, and 4.40 ppm were assigned to *N*,*N*′,*N*′-trimethyl protons (e), methylene protons (d), and methine protons of quaternary ammonium substitutent (c). These additional peaks were in good agreement with the results reported for GTMAC-conjugated CS in the literature (Serra et al., 2009). Although the signals of methylene protons from citrate moieties (a) were overlapped with the signals of $H^{2'}$ and methylene protons of quaternary ammonium moieties (b), the XRD data, solubility and thermal property (will be discussed later) provided the convincing evidence for QCDCA-*g*-CS formation.

Fig. 4 shows the water solubility test of QCS, and QCDCA-*g*-CS derivatives. It was found that CDCA-*g*-CS with various grafting percentages (22, and 36) was not dissolved in water regardless of the concentration and time (data not shown), while their quaternary ammonium derivatives were well dissolved in the same conditions. Since the positively charged trimethylated ammonium groups could easily solvate and attract the partially negative oxygens in H_2O. Moreover, these groups would also reduce the inter- and/or intramolecular hydrogen bonding between CS chains, resulting in the greater solubility. It was found that the transmittances were in the order of QCS > QCDCA22-*g*-CS > QCDCA36-*g*-CS at the corresponding concentrations. These results were in good agreement with DQ value. Therefore, the conjugation of GTMAC to the CS backbone increased in the water solubility of the original CS.

In addition, a powder X-ray diffraction (PXRD) analysis was performed to study the crystallinity of CS, QCS, and QCDCA-*g*-CS derivatives (Fig. 5). Crystallographic data of CS demonstrated the characteristic peaks around 10° and 20°. In general, CS was crystalline because of the strong intermolecular interaction between CS chains through intermolecular hydrogen bonding. The introduction of quaternary ammonium salts into CS chains would lead to a reduction in the intermolecular interaction between CS chains due to the electrostatic repulsion by the positively charged trimethylated ammonium groups of the modified CS. Thus, the crystalline of QCS decreased comparing to that of the parent CS. After CD grafting, the crystallinity of original CS was also destroyed according to the electrostatic repulsion between the positively charged trimethy-

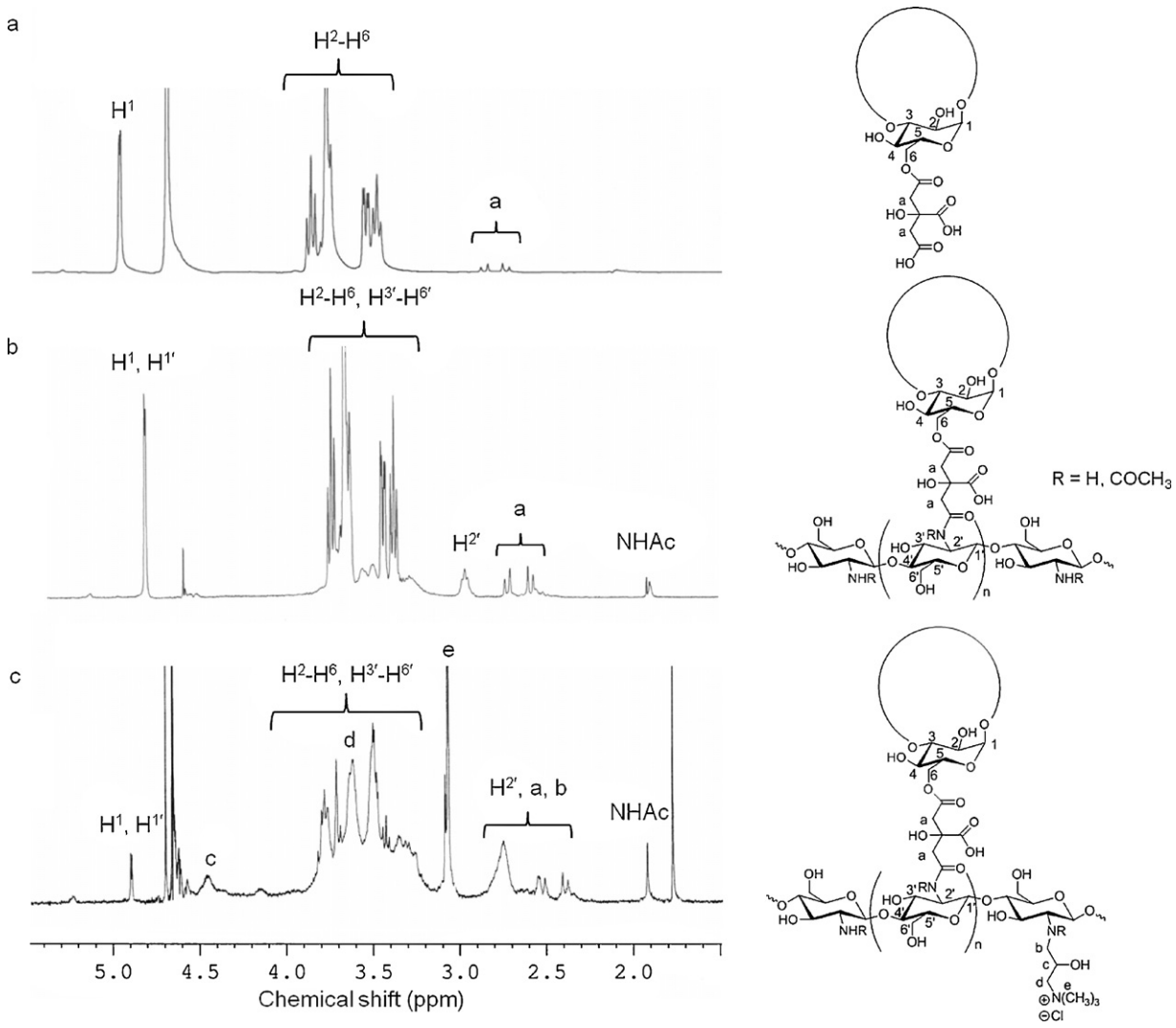

Fig. 3. Partial ^{1}H NMR spectra of (a) β-cyclodextrin citrate, (b) β-cyclodextrin-*g*-chitosan at 22% grafting, and (c) cationic β-cyclodextrin-*g*-chitosan at 22% grafting.

lated ammonium groups of the QCDCA-*g*-CS derivatives as well as the steric hindrance from CD moieties. This data indicated that the QCDCA-*g*-CS derivatives would be more amorphous in nature, which could improve the biodegradability and mucoadhesive properties of CS (Prabaharan & Gong, 2008).

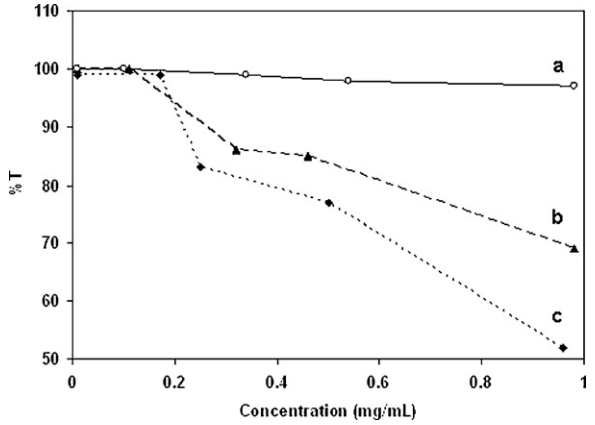

Fig. 4. UV–visible absorbance measurements of QCDCA-CS derivatives (a) cationic chitosan, (b) cationic β-cyclodextrin-*g*-chitosan at 22% grafting, and (c) cationic β-cyclodextrin-*g*-chitosan at 36% grafting.

Their thermal properties were also conducted. Differential thermal analysis curves of corresponding compounds were shown in Supplementary data. Two exothermic peaks were attributing to the loss of water and the heat decomposition of CS backbone. The lower decomposition temperature of QCS and QCDCA-*g*-CSs related to the decomposition of less organized CS molecules due to both electrostatic repulsion between the positively charged trimethylated ammonium groups of the GTMAC-conjugated CS and interruption of CD moieties on intermolecular hydrogen bonding of each CS chain.

3.4. Evaluation of mucoadhesive properties

3.4.1. Mucin-particle method

Mucoadhesive mechanism has been proposed based on 5 theories: wetting, adsorption, diffusion, electrical and fracture theories (Smart, 2005). The electrical theory can be determined by mucin-particle method. Initially, the particle size of the mucin particles was in the range of 250–300 nm with surface charges of −13 to −16 mV. At pH 6.8, PAA is fully ionized and confers a net negative charge. The electrostatic interaction between PAA and mucin with the same charge is generally repulsive. PAA was then tested as the negative control. Fig. 6 displays the particle size and zeta potential of the mucin particles when mixed with the various concentra-

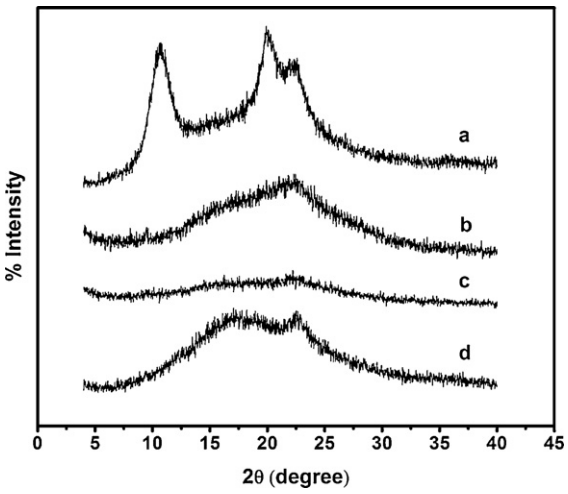

Fig. 5. X-ray diffraction patterns of (a) chitosan, (b) cationic chitosan, (c) cationic β-cyclodextrin-*g*-chitosan at 22% grafting, and (d) cationic β-cyclodextrin-*g*-chitosan at 36% grafting.

tions of the polymers. No significant change in mucin particle size and surface charge was observed (Fig. 6b) indicating the electrostatic repulsion with the same charges of PAA and mucin particles. For QCS, increasing in polymer concentration resulted in a significant increase in mucin particle size (Fig. 6c). The negatively charged mucin particles were neutralized and changed to positive upon the addition of QCS. The rationale of these changes is possibly due to the strong interaction between the positively charged QCS and the negatively charged mucin particles through electrostatic interaction, leading to polymer adsorption, and entanglement onto mucin particles. The large particle size and aggregation were consequently observed. This result was in accordance with our previous finding (Sajomsang, Ruktanonchai, Gonil, & Nuchuchua, 2009) and data reported by Sandri et al. (2005).

Similar result was found on QCDCA22-*g*-CS (Fig. 6e). Since CD itself has no interaction with mucin particles (as shown in Fig. 6a), the strong interaction between QCDCA22-*g*-CS and mucin particles would be favorable through electrostatic interaction between positively charged amino groups of the cationic CS and the negatively charged sialic acid residue of mucin particles. Interestingly, an introduction of QCDCA36-*g*-CS did not cause any significant change on mucin particle size and surface charge (Fig. 6f). It was possibly due to the lower DQ value. Moreover, carboxylic acid groups located at the spacer of QCDCA36-*g*-CS would play a key role on this observation. The high grafting percentage provided the larger amount of CD and carboxylic acid groups at the spacer. Since carboxylic acid groups of citrate moieties have a p*K*a value of ~6.4, thus, these groups were dissociated well and generated carboxylate anion at the pH 6.8, which was above their p*K*a. Therefore, these carboxylate anions would most likely interfere the electrostatic attraction and repelled the negatively charged mucin particles, leading to the insignificant change in mucin particle size and surface charge. To confirm this hypothesis, various amounts of CDCA, and spacer units were mixed with mucin particles as shown in Fig. 6d. No particle aggregation and change of surface charge were observed. Hence, the presence of citrate spacer significantly influenced the electrostatic force between CS derivatives and mucin particles.

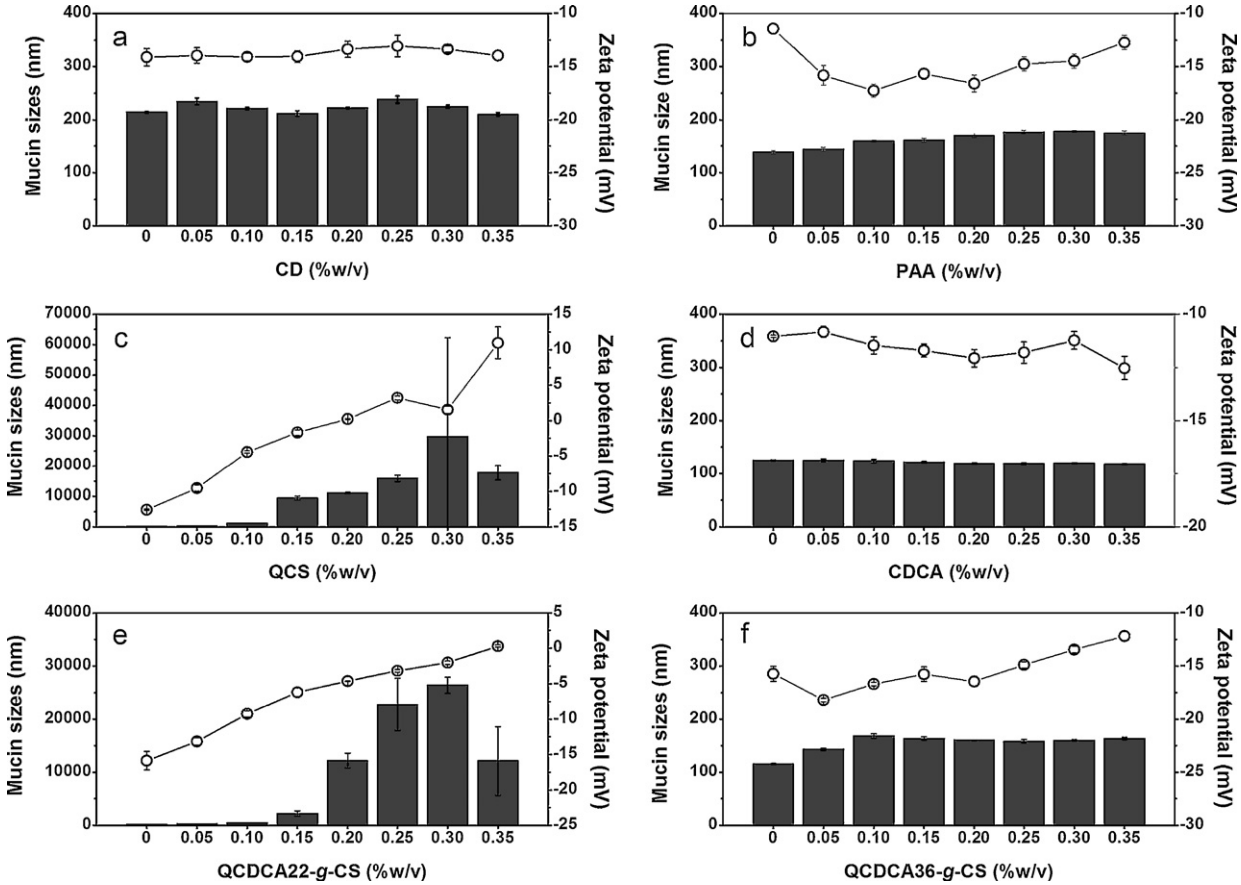

Fig. 6. The particle size (black bar) and zeta potential (○) of the mucin particles when mixed with the various concentrations of (a) β-cyclodextrin, (b) polyacrylic acid, (c) cationic chitosan, (d) β-cyclodextrin citrate, (e) cationic β-cyclodextrin-*g*-chitosan at 22% grafting, and (f) cationic β-cyclodextrin-*g*-chitosan at 36% grafting at pH 6.8.

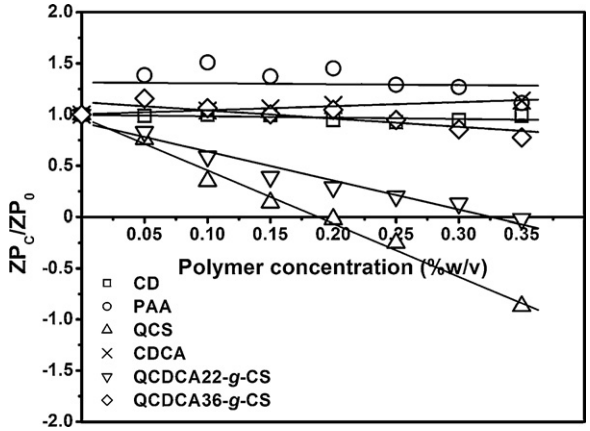

Fig. 7. The correlation of relative zeta potential (zeta potential at each polymer concentration (ZP_v)/zeta potential of the starting mucin particles (ZP_0)). Key: β-cyclodextrin (□); polyacrylic acid (○); cationic chitosan (△); β-cyclodextrin citrate (×); cationic β-cyclodextrin-*g*-chitosan at 22% grafting (▽); cationic β-cyclodextrin-*g*-chitosan at 36% grafting (◇).

Fig. 7 shows the correlation between the zeta-potential at various polymer concentrations and relative zeta-potential values (zeta-potential at each polymer concentration (ZP_c)/zeta potential of the starting mucin particles (ZP_0)). The critical concentration value of their polymers was evaluated by a linear equation when ZP_c/ZP_0 ratio equal to zero, indicating that mucin particles would be neutralized by an adsorption of the polymer molecules on their surface. The QCS provided the lowest critical concentration value, suggesting that less QCS was required to neutralize negatively charged mucin particles to be zero (Table 1). The higher the slope indicated the stronger the interaction. As expected, the QCS exhibited the highest slope value followed by QCDCA22-*g*-CS, while PAA, CD, and QCDCA36-*g*-CS showed the smaller values. This finding implied that QCS exhibited the highest electrostatic strength, according to the mucin-particle method.

Based on these results, it can be concluded that: (1) The QCS would be favorable for electrostatic attraction with negatively charged sialic acid and sulfonic acid residues of mucin particles though electrostatic interaction. (2) The electrostatic strength related to the DQ value.

3.4.2. SPR method

In addition to the electrostatic attraction (electronic theory), mucoadhesion can be mediated through various mechanisms, e.g., hydrogen bonding (Sogias, Williams, & Khutoryanskiy, 2008). To further investigate the mucoadhesive interaction of the QCDCA-*g*-CS, SPR technique, a well-known tool for monitoring biological interaction with biomaterials in real time (Green et al., 2000), was utilized in this study. Takeuchi et al. (2005) developed BIACORE method based on SPR technique for a detection and prediction of binding properties of mucoadhesive polymers. The mucoadhesion of polymers could be obtained in terms of refractive index change or RIU responses. If the binding between mucin particles and the polymers actually occurs, the response on surface of immobilized sensor will increase. The rate and the strength of binding can be determined from the slope and the value of the RIU response. The mucoadhesivity of QCDCA-*g*-CS derivatives was observed using QCS as a positive control. The sensorgrams were reported as Supplementary data.

Table 1
Critical concentration, percentage of RIU increase, and IC_{50} of various polymers.

Polymers	Critical concentration[a] (%, w/v)	%RIU increase[b]	IC_{50} value[c] (mg/mL)
PAA	1.56	–	–
CD	7.48	1.65 ± 0.42	12
QCS	0.18	75.57 ± 9.56	0.05
CDCA	2.52	−3.95 ± 0.22	0.25
QCDCA22-*g*-CS	0.33	87.51 ± 1.84	0.6
QCDCA36-*g*-CS	1.39	82.70 ± 3.71	0.15

[a] Evaluated by a linear equation when zeta-potential at each polymer concentration (ZP_c)/zeta potential of the starting mucin particles (ZP_0) ratio equal to zero.
[b] Determined by SPR method after injection of various polymer solutions at concentration of 0.5% (w/v) on mucin immobilized sensor chip.
[c] Determined from % relative cell viability of various polymer solutions on buccal mucosa cells.

The RIU response increased after mucin injection to the sensor chip surface. An increase in RIU response was due to the change of refractive index on the sensor chip surface according to the mucin immobilization. After the polymer introduction, the RIU response was found to increase for all samples. These results could be explained by the ability of the polymers to adhere on mucin-immobilized sensor chip, leading to the change of refractive index. The slopes of the sensorgrams after QCS and QCDCA-*g*-CS derivatives injection were similar for all cases. It can be implied that QCS and all derivatives interacted with mucin particles at the similar rate.

The changes of response after the injection of those derivatives were calculated as % RIU increased. The increasing values of RIU response were presented in Table 1. %RIU of QCS, QCDCA22-*g*-CS, and QCDCA36-*g*-CS were 75.57 ± 9.56, 87.51 ± 1.84, and 82.70 ± 3.71, respectively. However, those of CD and CDCA showed the insignificant change. It implied that both CD and CDCA cannot adhere onto and/or diffuse into mucin surface, which could be probably attributed to their low molecular weight. The results correspond well with mucin-particle method. In comparison with the parent QCS, both QCDCA22-*g*-CS and QCDCA36-*g*-CS provided the higher values. Although the QCDCA-*g*-CS derivatives showed the lower electrostatic effect than QCS according to the mucin-particle method, the carboxyl and hydroxyl groups from the spacer, which are known for their ability to form hydrogen bonding, may participate in the mucoadhesive interaction. These hydrogen bonds between carboxylate anion of QCDCA-*g*-CS derivatives at the spacers and mucus glycoprotein could enhance the mucoadhesivity together with electrostatic interaction between cationic CS base and negatively charged mucin particles, leading to the high mucoadhesivity.

Thus, the electrostatic attraction and hydrogen bonding were presumably attributed to the strong mucoadhesive of QCDCA-*g*-CS derivatives. However, based on mucin-particle method the carboxylate anions at the citrate spacer could also repulse the negatively charged mucin particles. Therefore, the amount of citrate spacer of QCDCA-*g*-CS is needed to be optimized in order to prevent the electrostatic repulsion and facilitate the mucoadhesion. The QCDCA22-*g*-CS provided the highest mucoadhesivity, which may be useful for the mucoadhesive drug delivery systems.

Based on mucin-particle method and SPR method, mucoadhesion can be mediated through (1) electrostatic interaction between cationic CS base and negatively charged mucin particles and (2) hydrogen bonds between carboxylate anion of QCDCA-*g*-CS derivatives at the spacers and mucus glycoprotein.

3.5. In vitro cytotoxicity study

The in vitro cytotoxicity of the QCS and QCDCA-*g*-CS derivatives against buccal mucosal cells was investigated and shown as IC_{50} values in Table 1. CD demonstrated as a safer material due to its high IC_{50} at 12 mg/mL whereas QCS was the most toxic among the observed materials with the IC_{50} of 0.05 mg/mL. The toxicity of QCS could possibly due to a presence of positively charged trimethylated ammonium groups. The IC_{50} values of

the QCDCA-*g*-CS derivatives was found in the order of QCDCA22-*g*-CS > QCDCA36-*g*-CS. This results suggest that low %grafted CS resulted in less toxic towards mucosal cells. The IC_{50} of CDCA was also evaluated in order to study the effect of carboxylic acid groups at the spacer. Interestingly, CDCA exhibited the high toxicity, which may attribute to the carboxylate anion. Thus, QCDCA36-*g*-CS provided the higher toxic as the larger amount of spacer units.

4. Conclusion

The water-soluble cationic QCDCA-*g*-CSs have successfully been synthesized through three steps: esterification of CD with citric acid, grafting with CS though citrate spacer, and quaternization with GTMAC. The CS derivatives were soluble in water under neutral or alkaline condition. In comparison with the parent CS, the considerable improvement in the mucoadhesive properties of QCDCA-*g*-CS derivatives was presumably based on the formation of electrostatic interaction between positively charged trimethylated ammonium groups of the QCDCA-*g*-CS derivatives and negatively charged sialic acid and sulfonic acid residues of mucin particles. Intermolecular hydrogen bonding between carboxylate anion of QCDCA-*g*-CS derivatives at the spacers and mucus glycoprotein was also favorable for strengthening the mucoadhesive interaction. The QCDCA-*g*-CS at 22% grafting showed the promising results in terms of mucoadhesivity and low toxicity, which could be potentially useful for mucoadhesive drug delivery systems.

Acknowledgements

This research was financially supported from the National Nanotechnology Center (NANOTEC), National Science and Technology Development Agency (NSTDA), Thailand (Project No. NN-B-22-EN4-94-51-10).

Appendix A. Supplementary data

Supplementary data associated with this article can be found, in the online version, at doi:10.1016/j.carbpol.2010.11.017.

References

Andrews, G. P., Laverty, T. P., & Jones, D. S. (2009). Mucoadhesive polymeric platforms for controlled drug deliver. *European Journal of Pharmaceutics and Biopharmaceutics*, *71*, 505–518.

Cardile, V., Frasca, G., Rizza, L., Bonina, F., Puglia, C., Barge, A., et al. (2008). Improved adhesion to mucosal cells of water-soluble chitosan tetraalkylammonium salts. *International Journal of Pharmaceutics, 362*, 88–92.

Chen, S., & Wang, Y. (2001). Study on β-cyclodextrin grafting with chitosan and slow release of its inclusion complex with radioactive iodine. *Journal of Applied Polymer Science*, *82*, 2414–2421.

Chiu, S.-H., Chung, T.-W., Giridhar, R., & Wu, W.-T. (2004). Immobilization of β-cyclodextrin in chitosan beads for separation of cholesterol from egg yolk. *Food Research International*, *37*, 217–223.

Cho, J., Grant, J., Piquette-Miller, M., & Allen, C. (2006). Synthesis and physicochemical and dynamic mechanical properties of a water-soluble chitosan derivative as a biomaterial. *Biomacromolecules*, *7*, 2845–2855.

El-Tahlawy, K., Gaffar, M. A., & El-Rafie, S. (2006). Novel method for preparation of β-cyclodextrin/grafted chitosan and it's application. *Carbohydrate Letters*, *63*, 385–392.

Furusaki, E., Ueno, Y., Sakairi, N., Nishi, N., & Tokura, S. (1996). Facile preparation and inclusion ability of a chitosan derivative bearing carboxymethyl-β-cyclodextrin. *Carbohydrate Letters*, *29*, 29–34.

Gaffar, M. A., El-Rafie, S. M., & El-Tahlawy, K. F. (2004). Preparation and utilization of ionic exchange resin via graft copolymerization of β-CD itaconate with chitosan. *Carbohydrate Letters*, *56*, 387–396.

Gomes, P., Gomes, C. A. R., Batista, M. K. S., Pinto, L. F., & Silva, P. A. P. (2008). Synthesis, structural characterization and properties of water-soluble N-(γ-propanoyl-amino acid)–chitosans. *Carbohydrate Letters*, *71*, 54–65.

Green, R. J., Frazier, R. A., Shakesheff, K. M., Davies, M. C., Roberts, C. J., & Tendler, S. J. B. (2000). Surface plasmon resonance analysis of dynamic biological interactions with biomaterials. *Biomaterials*, *21*, 1823–1835.

Hirai, A., Odani, H., & Nakajima, A. (1991). Determination of degree of deacetylation of chitosan by ^{1}H NMR spectroscopy. *Polymer Bulletin*, *26*, 87–94.

Huang, Y., Leobandung, W., Foss, A., & Peppas, N. A. (2000). Molecular aspects of muco- and bioadhesion: Tethered structures and site-specific surfaces. *Journal of Controlled Release*, *65*, 63–71.

Krauland, A. H., & Alonso, M. J. (2007). Chitosan/cyclodextrin nanoparticles as macromolecular drug delivery system. *International Journal of Pharmaceutics*, *340*, 134–142.

Lehr, C.-M., Bouwstra, J. A., Schacht, E. H., & Junginger, H. E. (1992). In vitro evaluation of mucoadhesive properties of chitosan and some other natural polymers. *International Journal of Pharmaceutics*, *78*, 43–48.

Liu, L., & Zhu, S. (2007). A study on the supramolecular structure of inclusion complex of β-cyclodextrin with prazosin hydrochloride. *Carbohydrate Letters*, *68*, 472–476.

Ludwig, A. (2005). The use of mucoadhesive polymers in ocular drug delivery. *Advanced Drug Delivery Reviews*, *57*, 1595–1639.

Marques, H. M. C., Hadgraft, J., & Kellaway, I. W. (1990). Studies of cyclodextrin inclusion complexes I. The salbutamol–cyclodextrin complex as studied by phase solubility and DSC. *International Journal of Pharmaceutics*, *63*, 259–266.

Martel, B., Devassine, M., Crini, G. G., Weltrowski, M., Bourdonneau, M., & Morcellet, M. (2001). Preparation and sorption properties of a cyclodextrin-linked chitosan derivative. *Journal of Polymer Science A: Polymer Chemistry*, *39*, 169–176.

Prabaharan, M., & Gong, S. (2008). Novel thiolated carboxymethyl chitosan-g-β-cyclodextrin as mucoadhesive hydrophobic drug delivery carriers. *Carbohydrate Letters*, *73*, 117–125.

Prabaharan, M., & Jayakumar, R. (2009). Chitosan-graft-β-cyclodextrin scaffolds with controlled drug release capability for tissue engineering applications. *International Journal of Biological Macromolecules*, *44*, 320–325.

Prabaharan, M., & Mano, J. F. (2006). Chitosan derivatives bearing cyclodextrin cavities as novel adsorbent matrices. *Carbohydrate Letters*, *63*, 153–166.

Sajomsang, W., Ruktanonchai, U. R., Gonil, P., & Nuchuchua, O. (2009). Mucoadhesive property and biocompatibility of methylated N-aryl chitosan derivatives. *Carbohydrate Letters*, *78*, 945–952.

Salamat-Miller, N., Chittchang, M., & Johnston, T. P. (2005). The use of mucoadhesive polymers in buccal drug delivery. *Advanced Drug Delivery Reviews*, *57*, 1666–1691.

Sandri, G., Rossi, S., Bonferoni, M. C., Ferrari, F., Zambito, Y., Di Colo, G., et al. (2005). Buccal penetration enhancement properties of N-trimethyl chitosan: Influence of quaternization degree on absorption of a high molecular weight molecule. *International Journal of Pharmaceutics*, *297*, 146–155.

Serra, L., Doménech, J., & Peppas, N. A. (2009). Engineering design and molecular dynamics of mucoadhesive drug delivery systems as targeting agents. *European Journal of Pharmaceutics and Biopharmaceutics*, *71*, 519–528.

Shumaker-Parry, J. S., Ruedi, A., & Campbell, C. T. (2004). Parallel, quantitative measurement of protein binding to a 120-element double-stranded DNA array in real time using surface plasmon resonance microscopy. *Analytical Chemistry*, *76*, 2071–2082.

Smart, J. D. (2005). The basics and underlying mechanisms of mucoadhesion. *Advanced Drug Delivery Reviews*, *57*, 1556–1568.

Snyman, D., Hamman, J. H., Kotze, J. S., Rollings, J. E., & Kotzé, A. F. (2002). The relationship between the absolute molecular weight and the degree of quaternization of N-trimethyl chitosan chloride. *Carbohydrate Letters*, *50*, 145–150.

Sogias, I. A., Williams, A. C., & Khutoryanskiy, V. V. (2008). Why is chitosan mucoadhesive? *Biomacromolecules*, *9*, 1837–1842.

Takeuchi, H., Thongborisute, J., Matsui, Y., Sugihara, H., Yamamoto, H., & Kawashima, Y. (2005). Novel mucoadhesion tests for polymers and polymer-coated particles to design optimal mucoadhesive drug delivery systems. *Advanced Drug Delivery Reviews*, *57*, 1583–1594.

Teijeiro-Osorio, D., Remuñán-López, C., & Alonso, M. J. (2009). Chitosan/cyclodextrin nanoparticles can efficiently transfect the airway epithelium in vitro. *European Journal of Pharmaceutics and Biopharmaceutics*, *71*, 257–263.

Thanou, M. M., Kotzé, A. F., Scharringhausen, T., LueBen, H. L., de Boer, A. G., Verhoef, J. C., et al. (2000). Effect of degree of quaternization of N-trimethyl chitosan chloride for enhanced transport of hydrophilic compounds across intestinal Caco-2 cell monolayers. *Journal of Controlled Release*, *64*, 15–25.

Thongborisute, J., & Takeuchi, H. (2008). Evaluation of mucoadhesiveness of polymers by BIACORE method and mucin-particle method. *International Journal of Pharmaceutics*, *354*, 204–209.

Tojima, T., Katsura, H., Han, S.-M., Tanida, F., Nishi, N., Tokura, S., et al. (1998). Preparation of an cyclodextrin-linked chitosan derivative via reductive amination strategy. *Journal of Polymer Science A: Polymer Chemistry*, *36*, 1965–1968.

Trapani, A., Sitterberg, J., Bakowsky, U., & Kissel, T. (2009). The potential of glycol chitosan nanoparticles as carrier for low water soluble drugs. *International Journal of Pharmaceutics*, *375*, 97–106.

Ugwoke, M. I., Agu, R. U., Verbeke, N., & Kinget, R. (2005). Nasal mucoadhesive drug delivery: Background, applications, trends and future perspectives. *Advanced Drug Delivery Reviews*, *57*, 1640–1665.

Venter, J. P., Kotzé, A. F., Auzély-Velty, R., & Rinaudo, M. (2006). Synthesis and evaluation of the mucoadhesivity of a CD–chitosan derivative. *International Journal of Pharmaceutics*, *313*, 36–42.

Zha, F., Li, S., & Chang, Y. (2008). Preparation and adsorption property of chitosan beads bearing β-cyclodextrin cross-linked by 1,6-hexamethylene diisocyanate. *Carbohydrate Letters*, *72*, 456–461.

Zhang, X., Wang, Y., & Yi, Y. (2004). Synthesis and characterization of grafting cyclodextrin with chitosan. *Journal of Applied Polymer Science*, *94*, 860–864.

Zhang, X., Wu, Z., Gao, X., Shu, S., Zhang, H., Wang, Z., et al. (2009). Chitosan bearing pendant cyclodextrin as a carrier for controlled protein release. *Carbohydrate Letters*, *77*, 394–401.